Low-Cost, High-Efficiency Quasi-Planar Array of Waveguide-Fed Circularly Polarized Microstrip Antennas

Mahmoud Shahabadi, Dan Busuioc, *Student, IEEE*, Amir Borji, *Member, IEEE*, and Safieddin Safavi-Naeini, *Member, IEEE*

Abstract—A low-cost quasiplanar *Ku*-band array of circularly polarized microstrip antennas benefiting from a low-loss waveguide feed network is demonstrated (patent pending). The 32 elements of the array which are arranged in a 2-by-16 configuration are subdivided into four two-by-four subarrays. To maintain feed losses and thus the overall noise temperature at a minimum, the subarrays are excited using a one-by-four corporate feed network of hollow metallic waveguides. This network is composed of *E*-plane components such as Tee-junctions and bends and is manufactured out of only two metallic pieces that accommodate the feed network in the form of milled grooves. Because of insensitivity of the exploited *E*-plane components to air gaps or slight misalignments, the pieces are secured together with only four screws without welding, braising, or conducting adhesives.

Owing to a low-loss foam substrate, the array elements show high circular polarization gain of 9 dBic and wide relative bandwidth of 4%. To achieve circular polarization, use is made of circular patches with two nearly perpendicular perturbations. Using sequential rotation of the elements along with quadrature phase shifting, the axial ratio of the array is reduced to 1 dB over 4% of bandwidth. The measured circular polarization gain of the array amounts to 23 dBic with an aperture efficiency of 63% in the *Ku*-band of frequencies. The achieved efficiency, which is higher than the reported efficiency for comparable planar arrays with microstrip feed networks, can be credited to the low losses of only 0.2 dB in its waveguide corporate feed. The paper also presents measurement results for an arrangement of two inclined single arrays mounted in parallel. This configuration which has a measured circular polarization gain of 25.7 dBic with an axial ratio of 1 dB is desirable for mobile low-profile antenna systems.

Index Terms—Circularly polarized microstrip antennas, foam substrates, high aperture efficiency, waveguide-fed arrays.

I. INTRODUCTION

MICROSTRIP antenna arrays are exploited in a vast number of engineering applications owing to their ease of manufacturing, low cost, low profile, and light weight, to name a few. In many practical designs, the elements of such arrays are fed by a coplanar corporate microstrip feed network in order to keep the overall constructional complexity at a minimum and maintain compact size [1]. At higher microwave frequencies, this approach, however, suffers from ohmic and dielectric losses of the connecting microstrip lines, as well as the undesired radiation of the feed network [1], [2]. Realization of a high-efficiency microstrip antenna array having a large number of elements can thus be challenging, unless a low-loss low-radiation feed network replaces the coplanar one.

To this end, the feed network should be a circuit of low-loss transmission lines. Among all microwave transmission lines, hollow metallic waveguides feature extremely low losses up to very high frequencies provided that their internal surfaces are finished smoothly. For this reason, they have been intensively utilized in the special feed system of planar slot arrays [3], [4] and in the beam forming network (BFN) of satellite antennas [5]. In [6]–[8] a waveguide structure is used to realize the corporate feed network of low profile arrays for mm-wave applications.

Waveguide feed networks have also been combined with microstrip antenna arrays to enhance the overall radiation efficiency of the resulting hybrid arrays. For instance, in [9], a waveguide with equidistant longitudinal slots excites several rows of microstrip lines feeding the radiating elements of a 77 GHz array. This method simplifies the feed network and at the same time provides a low-loss power distribution among the rows although its resonant nature reduces the operating bandwidth. Another example of a hybrid array is presented in [10] where a corporate feed network made of E-plane tees is used to excite 2×2 slot-coupled subarrays of linearly-polarized microstrip antennas.

The present work concerns with the realization of a *Ku*-band array of circularly polarized microstrip antennas profiting from a low-loss waveguide feed network. This network comprises of rectangular waveguides with E-plane tees and bends which form a novel, ultracompact corporate feed for the microstrip array. Since only E-plane components are exploited in the feed network, it is manufactured from two waveguide halves that are secured together with the help of a small number of screws. Unlike the waveguide-fed arrays introduced in [9], [10], no conductive adhesive is needed. Electromagnetic coupling between the waveguide feed network and the radiating elements is established using a low loss design for waveguide-to-microstrip transitions using coaxial probes.

Although the main concepts used in this research are well established, to the best knowledge of the authors, a practical and efficient design methodology for the entire waveguide-fed
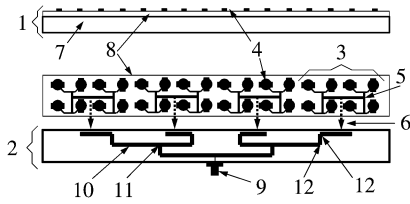
Fig. 1. Constituting components of the 2×16 array.

Fig. 2. Array element. (a) Top-view. (b) Side-view showing its two-layer substrate.

Fig. 3. Simulated single element radiation. E_{RHCP} and E_{LHCP} shown in solid and dashed lines, respectively.

microstrip array has not been published. Additionally, the ultracompact size, high efficiency, and modularity of the array structure lends itself to state-of-the-art consumer applications for home and mobile *Ku*-band satellite reception.

To introduce various components of the realized planar array, the paper is organized as follows. In Section II, the circularly polarized radiating elements and their subarrays are in focus, while the configuration of the waveguide feed network as well as the waveguide-to-microstrip transition are discussed in Section II-D. Radiation measurements conducted on the realized array are presented in Section III.

II. ARRAY CONFIGURATION

Fig. 1 illustrates the constituting components of the waveguide-fed planar array. It is composed of a two-layer substrate (1) for supporting the array elements and a waveguide feed network (2). The 32 elements of the array are subdivided into four subarrays of elements (3). Each element of the array (4) is a circularly polarized microstrip antenna in the form of a circular patch with stubs and notches as described in the following subsection. A microstrip corporate feed (5), the structure of which will be introduced shortly, connects a set of eight elements to form a subarray. The electrical connection of the four subarrays to the waveguide feed network is established through four waveguide-to-microstrip transitions (6).

A. Array Elements

Fig. 2(a) and (b) depict the top and side-view of a single array element, respectively. The circular shape of the element lends itself to independent excitation of two perpendicular modes when a microstrip line feeds the element at an angle of $45°$ as can be seen in Fig. 2(a). For this excitation, the polarization of the
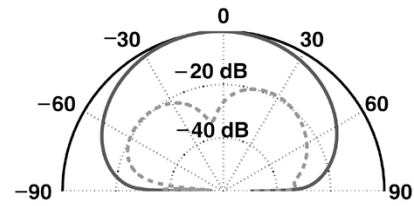
far-field electric field of these two modes will be E_H and E_V as illustrated in Fig. 2(a). Obviously, to achieve circular polarization, these modes must be excited with quadrature phase. For relatively narrow-band applications, the required phase shift can be implemented by a slight shift in the resonance frequencies of the two perpendicular modes. To shift these resonance frequencies to a slightly higher or a lower frequency and thereby to achieve the desired phase shift, the element layout of Fig. 2(a) is equipped with notches and stubs. Their relative orientation specifies relative phase shift between E_H and E_V, thus the sense of radiated circular polarization. For instance, the configuration shown in Fig. 2(a) radiates right-hand circular polarization. This can be changed to left-hand circular polarization if the notches switch their location with the stubs.

The substrate of the array elements is constituted of two layers. To achieve a wider bandwidth and a higher gain, the main substrate of the element is chosen to be a low-loss foam substrate (7) with a dielectric constant of $\epsilon_r = 1.047$ and a loss tangent of 0.0017 at 10 GHz. The thickness of this substrate amounts to 1.5 mm (0.0625λ). The array elements are printed on a 0.1 mm (0.004λ) thin FR4 substrate (8) stacked on the above mentioned foam layer.

To design the array elements, we have taken advantage from Agilent Momentum which applies the method of moments to the mixed-potential integral equation (MPIE) of multilayer media. In a first step, after setting up the two-layer substrate in Agilent Momentum, the layout of the element is parameterized by its radius, dimensions of its stubs and notches as well as their rotation angles around the element center. For any specific set of parameters, Agilent Momentum numerically computes the input impedance and radiation characteristics of the element. To guarantee the desired performance over bandwidth of interest, gain and axial ratio (AR) are calculated in the entire bandwidth. Optimum parameters are selected after searching for maximum gain and minimum AR of the element among the obtained numerical results. According to these results, the optimum element can have a gain of 9 dBic and an AR of smaller than 3 dB over a relative bandwidth of 4%. A polar plot showing the simulated normalized radiation pattern of E_{RHCP} and E_{LHCP} for the single optimized element is given in Fig. 3. High isolation of more than 20 dB between the two polarizations has been achieved. Additionally, the AR for the single element is given in Fig. 4. In the working bandwidth, a return loss of better than 17 dB has been achieved on the 170 Ω-input microstrip line.

B. Sequential Rotation

Although the achieved element gain is satisfactory, the axial ratio of 3 dB can be marginal in some applications. To further
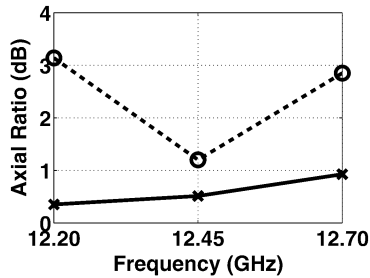
Fig. 4.   Simulated axial ratio of single element (dashed line) and of 2×1 sequentially rotated dual element (solid line).
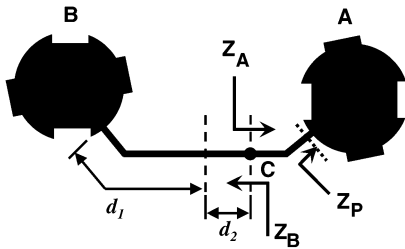

Fig. 6.   Simulated dual element radiation. E_{RHCP} and E_{LHCP} are shown in solid and dashed lines, respectively.

Fig. 5.   Sequential rotation. A: basic array element. B: basic element after $90°$ spatial rotation. C: excitation point.

Fig. 7.   Subarray of 2×4 elements made of four building blocks and a corporate microstrip feed network. Each building block "A" is constituted of a pair of elements. The corporate microstrip feed network is excited at its center point "B" so that the input power is equally distributed among all the elements.

improve the axial ratio, we have used two elements with sequential rotation of $90°$ in space. This spatial rotation must be compensated for by an electrical phase shift of $90°$ to retain circular polarization and to achieve an axial ratio better than that of a single element. This technique of improving axial ratio has been previously described in [11], and recently been used for similar array applications in [12], [13].

Fig. 5 shows a pair of elements after introduction of sequential rotation. The elements are connected together via a microstrip line of length $2d_1$ which includes a $45°$ bend at the input of each element, causing a slight mismatch looking into each of the elements. As can be seen in Fig. 5, the excitation point on this microstrip line is offset by d_2 from center. In order to obtain a purely resistive load at the driving point (C) of the pair of elements, the impedance levels Z_A and Z_B seen to the right and left of C must satisfy $Z_A = Z_B^*$. Additionally, in order to obtain the $90°$ electrical phase shift required, a secondary condition of $2\beta d_2 = \pi/2$ must be simultaneously satisfied.

Therefore, the two requirements of equal power distribution and quadrature phase shift uniquely determine d_1 and d_2. In some cases the obtained values for these parameters may lead to an inter-element spacing greater than the spacing required for maximizing the array factor, in which case the elements can be brought closer by slightly curving the connecting microstrip line.

Following the above procedure, we have designed the layout of a pair of elements. This layout has been imported into Agilent Momentum for final verification using the method of moments. The numerical results generated by Agilent Momentum have confirmed a significant improvement of axial ratio. A polar plot showing the simulated normalized radiation pattern of E_{RHCP} and E_{LHCP} for the designed element pair including the effect of the microstrip line connecting the two elements is given in Fig. 6. Additionally, the a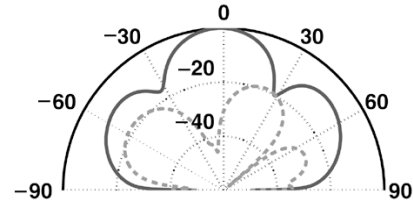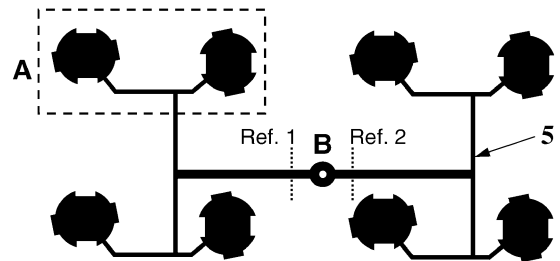xial ratio for the sequentially-rotated element pair is given in Fig. 4. It has been observed that the designed two-element array has an AR of only 1 dB over a relative bandwidth of 4%. In addition, a gain improvement of almost 3 dB has been achieved for the two-element array.

The optimized pair of two elements has then been used as a building block for formation of a 2×4 subarray. This is illustrated in Fig. 7. Here, a microstrip corporate feed network (5) equally distributes the input power among the four element pairs A. To this end, the electrical length of the microstrip lines connecting the element pairs A to the feed network input B are chosen equal. Obviously, in each section of the corporate feed, the characteristic impedance of the microstrip lines, therefore their line width, assumes different values to maintain optimum input matching for the desired bandwidth.

C. Waveguide-To-Microstrip Transition

To minimize feed losses, the input to the 2×4 subarray introduced in the previous Section is chosen to be a hollow rectangular waveguide. Considering the total thickness shown in Fig. 8(b), a coaxial-type transition is adopted instead of the aperture coupling proposed in [10]. The required transition from this waveguide to the microstrip corporate feed of the subarray (5) is illustrated in Fig. 8. It consists of a waveguide-to-coaxial transition followed by a coaxial-to-microstrip one. In the latter, as shown in Figs. 7 and 8(a), the two main microstrip lines of the feed emerge from the excitation point B which is connected to the center conductor of a TEM coaxial line. The three reference planes for the ports of this transition are specified in Fig. 8(b) as [1]–[3] whereas the ports of the next transition, i.e., from coaxial line to the waveguide, are on the planes denoted by [3], [4]. For the waveguide-to-coaxial transition, a probe suspended in a waveguide cavity is exploited according to Fig. 8(b) to convert the coaxial mode to the fundamental mode of the rectangular waveguide. Evidently, the cavity and probe dimensions as
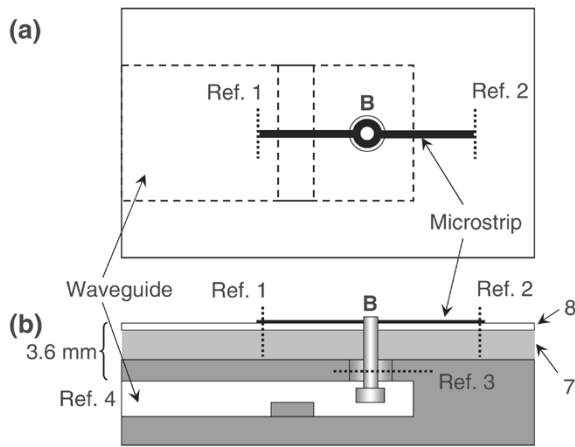
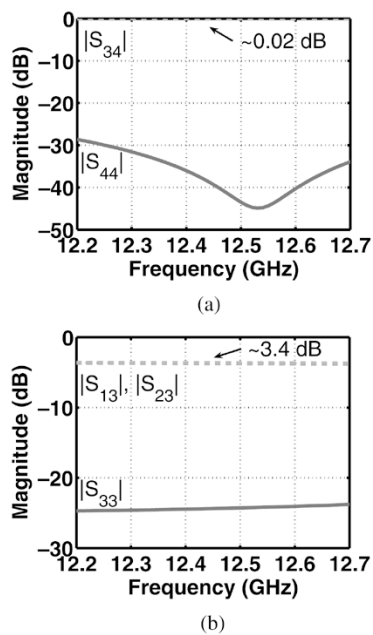Fig. 8. Waveguide-to-microstrip transition. (a) Top-view. (b) Cross section.

Fig. 9. Simulated waveguide-to-microstrip matching results. (a) Waveguide-to-coaxial. (b) Coaxial-to-microstrip.
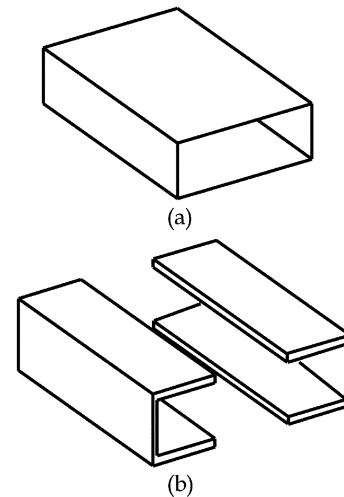

Fig. 10. (a) Hollow metallic waveguide. (b) Realization of waveguide using two metallic blocks. After assembly, each of the grooves cut in the blocks form one half of the internal space of the waveguide.

D. Feed Network of Hollow Metallic Waveguides

The antenna array consists of four 2×4 subarrays of the type described above. Considering microstrip feed losses which are naturally higher than waveguide, the 2×4 subarray represents the highest number of elements which can be fed entirely in microstrip, before the loss incurred by further microstrip feed lines diminishes the performance obtained by an increase in the number of elements.

Therefore, in order to feed the four input waveguides of these microstrip subarrays with minimum losses and thus maximum efficiency, a 1: 4 power dividing network of hollow metallic waveguides has been exploited. This network is composed of reduced-height waveguide components, and represents a compromise between lower losses and higher physical size, which are inherent to waveguide technology. The input to the network is a high-frequency coaxial connector of SMA type [(9) in Fig. 1] whereas its four outputs are the input waveguides of the subarrays.

The waveguide components used in the feed network are of E-plane type. The reason for preferring E-plane to H-plane components is their ease of manufacturing. More specifically, a hollow metallic waveguide, such as the one seen in Fig. 10(a), can be divided into two halves along the principal E-plane of the waveguide according to Fig. 10(b). Either of these parts is manufactured out of a metallic block by milling grooves that after assembly form the hollow internal space of the waveguide. It is worth mentioning that possible air gaps incurring after assembling the two blocks have minor effect on the performance of the waveguide because they appear along the principal E-plane of the waveguide where surface current on the waveguide top and bottom wall is solely longitudinal, i.e., in parallel to the gaps. If the principal H-plane of the waveguide were selected as the cut plane to divide it into two halves, possible air gaps after assembly would negatively affect waveguide functionality since the surface current on the waveguide side walls are perpendicular to the principal H-plane. The above mentioned advantage of E-plane to H-plane section also explains why small amount

well as microstrip line width are to be determined for maximum transmission in the given bandwidth.

For this purpose, Ansoft HFSS, a simulation tool founded on the method of finite elements is utilized. Using sweep facility of this tool, one can perform separate full-wave analysis of the two transitions for a variety of different dimensions assigned to the cavity, probe, and microstrip lines. The optimum dimensions corresponding to the maximum cascaded transmission coefficient can be searched for among the swept values. After selection of the optimum dimensions among the swept values, the scattering parameters of the waveguide-to-coaxial and coaxial-to-microstrip transitions were separately evaluated. These are presented in Fig. 9(a) and (b), respectively. They confirm that losses in power transfer from the input waveguide to the microstrip feed network of the subarray can be as low as 0.4 dB over 4% bandwidth. Furthermore, once the optimum physical dimensions were determined, one simulation of the entire waveguide-to-microstrip transition was performed for verification.

of pressure and therefore small number of screws can be applied to the assembly of the proposed E-plane feed network.

To maintain the dimensions of the array at a minimum, the feed network exploits reduced-height waveguide components, indicated as (10) in Fig. 1. Evidently, other waveguide components are needed to implement the desired one-by-four corporate feed network. These are Tee-junctions (11) and bends (12) as depicted in Fig. 1. Compared to the work proposed in [10], the bends developed here help reduce the overall depth of the 2×16 array. Both Tee-junctions and bends are also chosen to be of E-plane type so that they can be manufactured as grooves cut in the two metallic blocks along with the other waveguide components described above. The overall electrical lengths of the four branches of the feed network are equal to maintain uniform phase distribution among the four outputs. Note that the unwanted phase inversion caused by the two E-plane Tee-junctions of the feed network is compensated in the two U-shaped sections of Fig. 1 where the polarity of the electric field is inverted.

The final structure of the feed network is designed with the help of Ansoft HFSS. For this purpose, geometrical features of the feed network along with the input and output coaxial lines are used to compose a model for Ansoft HFSS. To save on computational resources, only one half of the feed network appears in the model owing to the symmetry of the feed network. The objective function observed in the course of optimization includes both magnitude and phase of the transmission coefficients of the feed network, while the optimization goal is equalization of magnitude and phase among the four outputs. It should be added that some of the components of the feed network such as E-plane Tee-junctions, bends, or waveguide-to-coaxial transitions are designed and optimized separately before inclusion in the final model. After optimization, the transmission coefficients of the optimized feed network assume values within $-6.0\,\mathrm{dB} \pm 0.1\,\mathrm{dB}$ over a wide bandwidth. Moreover, the phase difference among the outputs of the optimized feed network is negligible. It should be emphasized that the performance of the feed network has been investigated numerically after assuming four ideal terminating loads at its output ports.

In the last stage of the realization of the feed network, the HFSS model of the optimized feed network has been converted to a data format readable by a computer numerically controlled (CNC) milling machine. Two data files are generated for this purpose. One of the data files has controlled the cutting tool during the milling of the grooves into one of the two aluminum blocks. The mirrored version of the grooves has been included in the second data file which has been used to mill the second aluminum block. Fig. 11 is a photo of the two metallic halves after CNC milling. The feed network formed by the grooves can be recognized in this photo. To assemble the feed network, the two metallic blocks are secured together using only four metallic screws.

III. MEASUREMENTS RESULTS

Fig. 12 shows the antenna array after attachment of the metallic feed network to the two-layer substrate supporting the

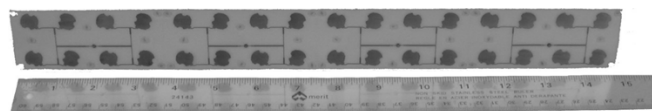Fig. 11. CNC-milled two-piece waveguide feed system.

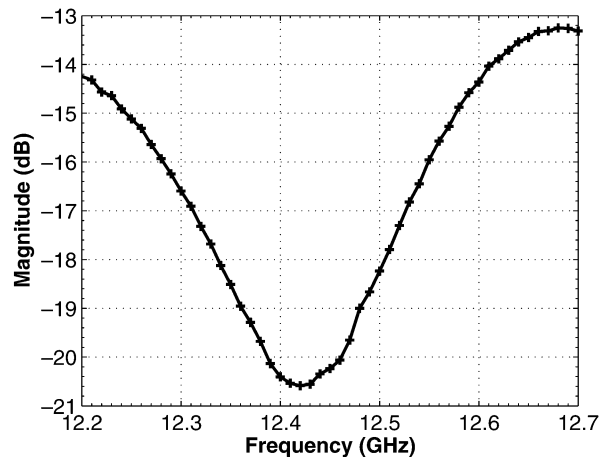Fig. 12. 2×16 complete manufactured antenna module.

Fig. 13. Measured input matching of 2×16 array.

array elements. As discussed below, to characterize the array, it is measured both as a stand-alone antenna and as a subarray in a dual configuration.

A. Stand-Alone Array

The input scattering parameter of the antenna array is measured and demonstrated in Fig. 13. It is apparent that a good matching is achieved over a wide range of frequencies. The presented results are obtained without any post-fabrication
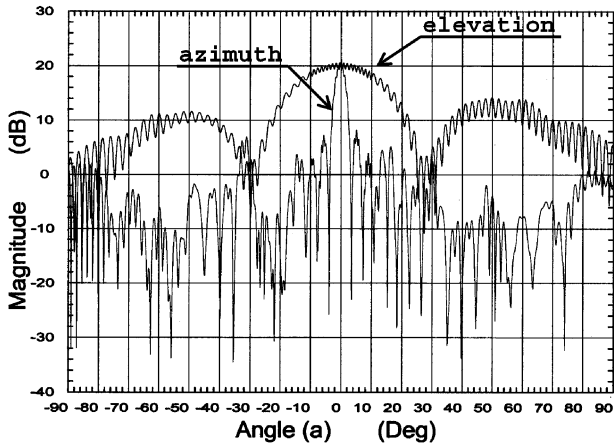
Fig. 14. Measured far-field spinning linear pattern of single 2×16 array. Frequency = 12.45 GHz.
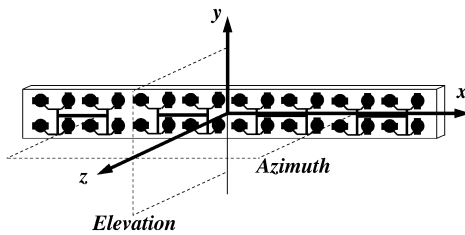

Fig. 15. Principal azimuth and elevation planes.

trimming—such as additional milling, or manufacturing of the waveguides or transition components.

The radiation characteristics of the array are measured using spinning linear patterns in the far-field region. Fig. 14 illustrates the results of these measurements in the principal azimuth and elevation planes of the array. These planes are defined in Fig. 15. From the spinning linear patterns the circular polarization gain of the array has been calculated to be 23 dBic at 12.45 GHz, with a half-power beam-width of the azimuth and elevation planes of 5.5° and 39°, respectively.

The simulated element gain of 9 dBic at the same frequency along with the fact that the array is composed of 32 elements can be used to estimate the array gain of 24 dBic under the assumption that the elements are excited using a loss-less uniform feed network with optimum inter-element spacing. The major cause of the above 1 dB difference between the estimated and measured gain can be attributed to conductor losses in the microstrip corporate feed of the subarrays and to the insertion loss of the waveguide-to-microstrip transition. As discussed earlier, the losses added by the waveguide feed network are estimated to be smaller than 0.2 dB, so they are considered as second-order causes. The other cause of lesser importance is element gain reduction due to inter-element interaction through the microstrip feed network of the last layer. Note that the relatively thick foam layer in the two-layer substrate of the array prevents any unwanted inter-element coupling through surface-wave modes because permittivity of the foam layer is close to unity.

The array axial ratio is also evaluated from the spinning linear pattern. This amounts to 1.0 dB at the working center frequency of 12.45 GHz. Measurements of three frequency points are summarized in Table I for circular polarized (CP) gain and AR.

TABLE I
KEY FEATURES OF HIGH-EFFICIENCY PLANAR ANTENNA WITH WAVEGUIDE FEED

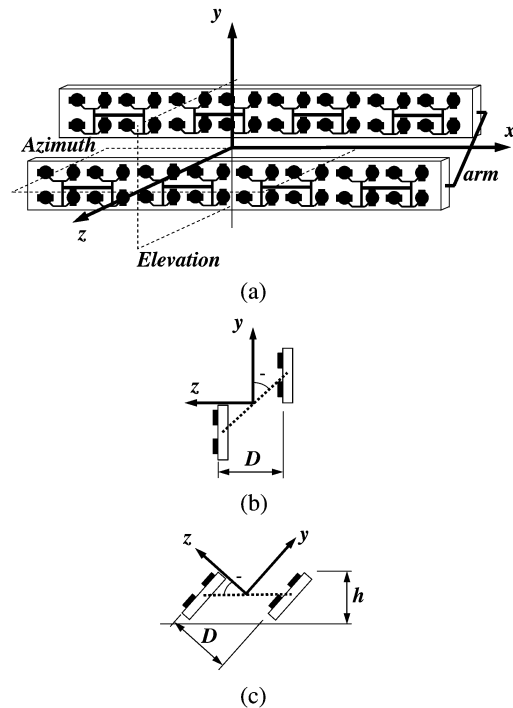| Frequency (GHz)	CP Gain (dB)	CP AR (dB)
12.20	22.64	1.10
12.45	23.02	1.05
12.70	22.32	0.83

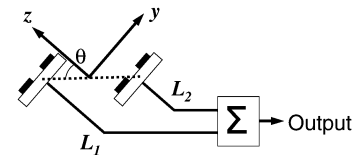Fig. 16. (a) Dual configuration. (b) Side view. (c) Side view after rotation.

Fig. 17. Combining array signals using unequal-length flexible cables and a passive one-by-two power combiner.

These results verify the effectiveness of the sequential rotation technique for AR improvement as described in Section II.

B. Dual Configuration

The prototyped antenna array can be exploited in the dual configuration illustrated in Fig. 16(a). While in this configuration the two arrays are in parallel, there is a certain amount of horizontal displacement between them. A supporting arm fixes the two arrays in the shown arrangement. The side-view of this configuration is drawn in Fig. 16(b). According to this drawing, the line connecting two similar points on the arrays makes an angle of θ with the y-axis. Rotating the arrays by θ, we arrive at the side-view of Fig. 16(c). The latter utilization lends itself to applications for which a low-profile construction is of prime importance. This is because the height h in Fig. 16(c) is almost one half of the height of a hypothetical array comprised of two
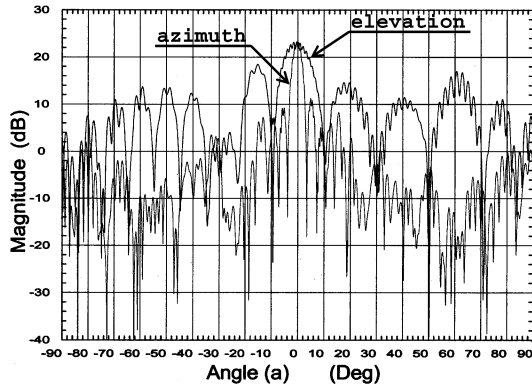
Fig. 18. Measured far-field spinning linear pattern of dual 2×16 array. Frequency $= 12.45$ GHz.

TABLE II
KEY FEATURES OF HIGH-EFFICIENCY PLANAR ANTENNA WITH WAVEGUIDE FEED

Feature	Specification
Frequency	12.2 - 12.7 GHz
Number of elements	2×16
Aperture size	$40 \times 366 mm$
Input matching	20 dB (@ 12.45 GHz)
Input connector	SMA
Circular polarization gain	23 dBic
Axial ratio	1.0 dB

TABLE III
SUMMARY OF LOSSES IN VARIOUS ARRAY COMPONENTS

Component	Loss (dB)
Microstrip feed	0.3
Microstrip-to-coaxial transition	0.4
Coaxial-to-waveguide transition	0.02
Waveguide corporate feed	0.2
Input connector	0.1

side-by-side arrays. For the configuration of Fig. 16(c), the main radiation lobe assumes a take-off angle of θ, which is another useful feature of this configuration because tilted main lobes can be advantageously exploited for low-profile base-station antennas of wireless links or for low-profile satellite terminals in which an inclined main lobe is desirable.

If the spacing of the two arrays, i.e., D in Fig. 16(b), is a multiple of the wavelength at the working frequency, one can combine the signal of the two arrays using equal-length microwave cables followed by a power combiner. However, this combination represents a narrow-band solution as for varying frequencies the spacing D corresponds to different electrical lengths. To overcome the mentioned chromatic error, unequal-length cables are used as shown in Fig. 17. Using this technique, the extra free-space propagation delay occurring for the back array is compensated for by the true-time delay in the longer cable of the front array. If the cable length difference $L_1 - L_2$ is chosen to be $v_p D/c$ in which v_p and c stand for the phase velocity in the cable and the light velocity in free space, respectively, a substantial improvement of the working bandwidth will be achieved. A more detailed analytical investigation carried out for three frequency points of the desired bandwidth can be used to determine the optimum length difference $L_1 - L_2$ for covering a given bandwidth.

Next, two arrays are arranged in the dual configuration for $\theta = 31°$. Flexible microwave cables (Semflex Company) and a commercial Ku-band power combiner (Atlantic Microwave Limited) are used to combine array outputs. For this arrangement, spinning linear patterns have been measured in the far-field zone and presented in the diagram of Fig. 18. The principal azimuth and elevation planes used during the measurements of Fig. 18 are defined in Fig. 16(a). According to the measurements results, a maximum gain of 25.7 dBic at 12.45 GHz has been achieved for the dual configuration which is slightly less than 3 dB enhancement over a single array gain. The half-power beam-width of the azimuth and elevation planes has been determined to be 5.25° and 16°, respectively. This can be attributed to cable and combiner insertion losses. As expected, grating lobes can be observed in the elevation plane pattern as the spacing D between the two arrays is greater than the free-space wavelength. The azimuth plane pattern does not show any significant deviation from that of a single array. Similarly, the axial ratio

of the dual configuration remains unchanged with respect to a single array and has the value of 1 dB.

IV. CONCLUSION

A low-cost quasiplanar Ku-band antenna array of high efficiency and small size is demonstrated (patent pending). It can be considered as transmit or receive unit for modular antenna systems that require a number of low-profile high-gain subarrays, such as land-mobile satellite terminals. Despite its small physical aperture of only 40×366 mm, its high efficiency enables this array to achieve a circular polarization gain of better than 23 dBic and an axial ratio of 1.0 dB in the Ku-band of frequencies. Table II summarizes the features of the developed array. Note that the losses involved in the waveguide feed network remain almost unchanged for a larger array size. Contrast this fact with the fact that the efficiency of a planar array with microstrip feed network decreases by increasing the array geometrical size [1], [10]. Moreover, since the feed network of the demonstrated antenna is comprised of E-plane bends and Tees, its sensitivity to assembly errors is minimal. Input interface to the array feed network is through a standard SMA connector with return loss better than 13 dB over a wide frequency band. The amount of loss in various array components is summarized in Table III.

A number of features distinguish this planar array from its counterparts, including the high aperture efficiency of 63%, as well as novel designs in the power distribution network. Additionally the modularity and high compact features of the 2-by-16 array are useful when contrasting this implementation to microstrip-only feed network arrays used in building larger-sized array systems.

It must be added that the concept of the feed system described in this paper can readily be applied to higher frequencies of millimeter waves without substantial modification. Due to its extremely low loss, the equivalent noise temperature of the array is low, which turns the introduced antenna array to a

suitable building block for antenna systems used in upcoming millimeter-wave satellite terminals.

ACKNOWLEDGMENT

REFERENCES

[1] P. S. Hall and C. M. Hall, "Coplanar corporate feed effects in microstrip patch array design," *Proc. Inst. Elect. Eng.*, pt. H, vol. 135, pp. 180–186, Jun. 1988.

[2] E. Levine, G. Malamud, S. Shtrikman, and D. Treves, "A study of microstrip array antennas with the feed network," *IEEE Trans. Antennas Propag.*, vol. 37, no. 4, pp. 426–434, Apr. 1989.

[3] S. R. Rengarajan, "Compound coupling slots for arbitrary excitation of waveguide-fed planar slot arrays," *IEEE Trans. Antennas Propag.*, vol. 38, no. 2, pp. 276–280, Feb. 1990.

[4] J. Hirokawa and M. Ando, "45 linearly polarized post-wall waveguide-fed parallel-plate slot arrays," *Proc. Inst. Elect. Eng. Microw. Antennas Propag.*, vol. 147, pp. 515–519, Dec. 2000.

[5] L. Accatino, B. Piovano, and G. Zarba, "Reduction in size and weight of waveguide beam forming networks for satellite applications," in *Proc. Antennas and Propagation Soc. Int. Symp.*, vol. 3, Jul. 1996, pp. 1996–1999.

[6] T. Sehm, A. Lehto, and A. V. Raisanen, "A large planar 39-GHz antenna array of waveguide-fed horns," *IEEE Trans. Antennas Propag.*, vol. 46, no. 8, pp. 1189–1193, Aug. 1998.

[7] K. Egashira, E. Nishiyama, M. Aikawa, K. Yoshiki, and S. Egashira, "Planar array antenna using waveguide-fed sub-array," in *Proc. 3rd Int. Conf. Microwave and Millimeter Wave Technology, ICMMT 2002*, 2002, pp. 592–595.

[8] C. Wu, "Low-Profile Waveguide Network for Antenna Array," U.S. Patent 6 563 398 B1, May 2003.

[9] F. Kolak and C. Eswarappa, "A low profile 77 GHz three beam antenna for automotive radar," in *Proc. Microwave Symp. Dig., 2001 IEEE MTT-S Int.*, vol. 2, 2001, pp. 1107–1110.

[10] W. Menzel, M. Schreiner, R. Mack, and P. J. N. Vera, "Millimeter-wave microstrip antenna arrays with waveguide feed network," *Frequenz*, vol. 55, pp. 11–12, 2001.

[11] P. S. Hall, "Review of techniques for dual and circularly polarized microstrip antennas," *Microstrip Antennas*, 1995.

[12] C. Wang and K. Chang, "A novel CP patch antenna with a simple feed structure," in *Proc. Antennas and Propagation Soc. Int. Symp.*, vol. 38, Jul. 2000, pp. 1000–1003.

[13] N. C. Karmakar and M. E. Bialkowski, "Circularly polarized aperture-coupled circular microstrip patch antennas for L-band applications," *IEEE Trans. Antennas Propag.*, vol. 47, no. 5, pp. 933–940, May 1999.

Mahmoud Shahabadi received the B.Sc. and M.Sc. degrees from the University of Tehran, Iran, and the Ph.D. degree from Technische Universitaet Hamburg-Harburg, Germany, all in electrical engineering in 1988, 1991, and 1998, respectively. Since 1998, he has been an Assistant Professor with the Department of Electrical and Computer Engineering, University of Tehran. From 2001 to 2004, he was with the Department of Electrical and Computer Engineering, University of Waterloo, Canada, as a Visiting Professor. Additionally he is a co-founder and CTO of MASSolutions Inc., a Waterloo-based company with a focus on advanced low-profile antenna array systems.

His research interests and activities encompass various areas of microwave and millimeter-wave engineering as well as photonics. Computational electromagnetics for microwave engineering and photonics find his special interest. He is currently conducting research and industrial projects in the field of antenna engineering, photonic crystals, left-handed materials, and holography.

Dr. Shahabadi was awarded the 1998/1999 Prize of the German Metal and Electrical Industries, Nordmetall, for his contribution to the field of millimeter-wave holography.

Dan Busuioc (S'96) received the B.Sc. and M.Sc. degrees in electrical engineering from the University of Waterloo, Waterloo, ON, Canada, in 2001 and 2002, respectively, where he is working toward the Ph.D. degree.

From 1996 to 2003, he has held a number of consulting engineering positions in Germany, the United States, and Sweden. He is a co-Founder and President/CEO of MASSolutions Incorporated, a Waterloo-based company focusing on advanced low-profile antenna array systems. Since 2004, he has been a Wireless Hardware Engineering Consultant with Teradyne Incorporated, Boston, MA. His research interests include novel antenna systems and novel high-frequency circuitry, including EBG/PBG antennas and feed systems. Additionally he has interest in the wireless systems and automated test equipment (ATE) industries.

Mr. Busuioc has been the recepient of the National Science and Engineering Research Council of Canada (NSERC) Industrial Postgraduate Scholarship in 2001 (with Ericsson Radio Access, Sweden) and in 2003 (with Winegard Company, Burlington, IA).

Amir Borji (S'99–M'04) was born in Tehran, Iran, in August 1971. He received the B.Sc. and M.Sc. degrees in electrical engineering from Isfahan University of Technology, Isfahan, Iran, in 1994 and 1998, respectively, and the Ph.D. degree in electrical engineering from University of Waterloo, Waterloo, ON, Canada in April 2004.

From January 1999 to April 2004, he was a Research Assistant in the Department of Electrical and Computer Engineering at the University of Waterloo, where since May 2004, he has been a Postdoctoral Fellow and CAD software consultant. His research interests include synthesis, design, and EM analysis of microwave filters, full-wave electromagnetic analysis of shielded structures using integral equation methods, and design and analysis of new planar EBG/PBG structures with applications in compact antenna arrays.

Dr. Borji was the recipient of the Ontario Graduate Scholarship award in 2002.

Safieddin Safavi-Naeini (S'75–M'78) received the B.Sc. degree in electrical engineering from the University of Tehran, Tehran, Iran, in 1974, and the M.Sc. and Ph.D. degrees in electrical engineering from the University of Illinois at Champaign-Urbana, in 1975 and 1979, respectively.

From 1980 to 1995, he was an Assistant Professor and then an Associate Professor with the Electrical Engineering Department, University of Tehran. In 1996, he joined the University of Waterloo, Waterloo, ON, Canada, where he is currently a Professor with the Department of Electrical and Computer Engineering. He has been a scientific and technical consultant to numerous national and international telecom industrial and research organizations over the last 20 years. He has authored or co-authored over 130 papers in technical journals and conferences. His research interests and activities include numerical electromatnetics applied to analysis and design optimization of RF/microwave/millimeter-wave systems and circuits, antenna and propagation, wireless communication systems, very high speed digital circuits, and photonics.